

ARTICLE

Binding Properties of CO, NO, and O₂ to P450 Heme: a Density Functional Study

Xiao-min Sun^a, Huan-jie Wang^b, Da-cheng Feng^{b*}*a. Environment Research Institute, Shandong University, Ji'nan 250100, China;**b. Institute of Theoretical Chemistry, Shandong University, Ji'nan, 250100, China*

(Dated: Received on January 3, 2006; Accepted on January 29, 2006)

The structural and binding properties of diatomic molecules CO, NO and O₂ to P450 heme were investigated in two different models (labeled as M1 and M2) using density functional method at the B3LYP/6-31G(d) level. The effects of the serine residue near diatomic molecules XO were considered in the model M2. The results show that the serine residue near the heme enforced the binding of XO to heme. Frequency analysis indicates that the stretching vibrational frequency decreased as CO, NO, and O₂ complex with heme.

Key words: P450 heme, Reaction mechanism, Density function theory

I. INTRODUCTION

Cytochrome P450 enzymes ubiquitously distributed in living things play important roles in the oxidation of a large variety of structurally diverse compounds including endogenous, physiological substrates and a wide range of drugs and xenobiotics, and its drug metabolism and involvement in brain chemistry make this enzyme a target for the drug industry and biomedical research [1]. O₂ is indispensable in the oxidation of substrates or xenobiotics through P450. CO is often used as an O₂ analogue for binding to the heme distal site [2,3]. It can bind strongly to Fe(II), and it is used in experiments on cytochrome oxidases to trap the enzyme in the fully reduced state [4]. Inhibition by CO is one of the hallmarks of processes catalyzed by P450, although many of the reactions catalyzed by biosynthetic P450 isozymes are relatively resistant to inhibition by CO [1]. The discrimination between O₂ and CO in P450 is of vital importance, accounting for wide variations in binding affinity, selectivity, and reactivity, and it has a strong impact on the metabolism of drugs and other xenobiotics. Understanding these interactions is of fundamental importance for elucidating the biological activities of heme proteins [5].

There have been numerous investigations on the interactions between diatomic molecules, such as CO, NO, and O₂ (labeled as XO, X=C, N, O) with heme [4-17], but most of them are about hemoglobin and myoglobin. The discrimination between O₂ and CO has been debated for decades. Collman *et al.* suggested that the discrimination between O₂ and CO when bound to the heme iron is achieved by steric repulsion [12,18], while Sigfridsson and Ryde concluded that electrostatics is the major source of myoglobin's discrimination

between O₂ and CO [6]. However, study on the discrimination between O₂ and CO by P450 hemoglobin is rare. Thus in this research, to investigate the difference of the O₂, NO, and CO binding P450 hemoglobin from the other hemoglobin and myoglobin, theoretical study on O₂, NO, and CO binding to P450 heme was carried out.

II. MODELS

In this study the crystal structure of CYP121, a mycobacterial P450 (PDB code 1n40 [19]), was used as a starting point (seen in Fig.1). Two models, labeled as M1 and M2, were used to study the different interactions between XO and heme. In model M1, the heme group was modeled as a porphyrin ring, the proximal cysteine (Cys345) was replaced by methyl mercaptide, and the system was the six-coordinated FeP(Cys)-XO (Cys=-SCH₃). In model M2, the heme group was modeled in the same way as in M1, but the proximal Cys345 was modeled as a -SC₂H₅ and the near amino acid residue serine (Ser237) is modeled as a CH₃CH₂OH with the α -carbon frozen relative to three carbons in the outer part of the porphyrin ring during the geometry optimization (seen in Fig.2, where the frozen atoms are marked with asterisks). This makes the distal serine more flexible and more capable of changing its hydrogen-bonding distance to the heme binding site ligand.

From Fig.1, it can be seen that the H atom of Ser237 form hydrogen bonds with the two O atoms of Oxy501. Hydrogen bonds are relatively weak interactions between molecules and yet they are of paramount importance in chemistry and pivotal in determining biomolecular structure and function [20]. This type of interaction governs many biologically important processes in which the enzymatic catalysis is particularly relevant [21-23]. The incipient stage in enzymatic catalysis is formation of the hydrogen bonds between enzyme and substrate or hydrogen bonds between the enzyme

* Author to whom correspondence should be addressed. E-mail: fdc@sdu.edu.cn

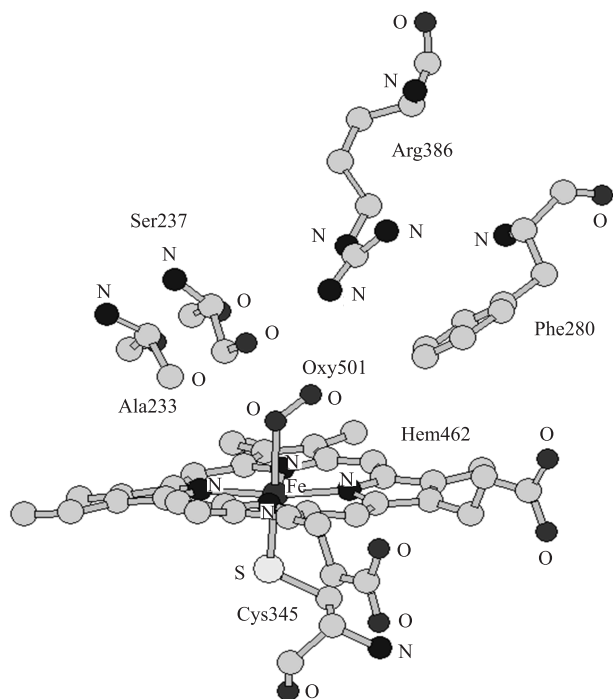


FIG. 1 The active site of the hemoglobin in PDB1n40.

residues. Taking account of the importance of the hydrogen bonds formed between Oxy501 and Ser237, the model M2 considering Ser237 has been put forward.

III. METHODS

The reason for the wide use of density functional method (DFT) is its high efficiency for large systems. DFT method has been proved to be a promising and successful method handling bioorganic systems [24]. Among the available density functional methods, the B3LYP method in particular seems to be the most widely used method and can give reliable results [25-27]. Therefore, in these calculations the geometries were optimized using the B3LYP method, which is the Becke's three parameter hybrid exchange functional combined with the Lee-Yang-Parr correlation functional. The basis set used is 6-31G(d). Frequency analysis at the same level was carried out on the optimized geometries to confirm that the obtained geometries are local minima. NBO analysis was also calculated on the optimized geometries. All calculations were performed using the Gaussian03 package.

The binding energy of XO to heme has been defined as the energy difference between the complex and the monomers. The basis set superposition effects (BSSE) should be considered when the intermolecular interactions are calculated. Then for the M1-XO system,

$$\Delta E(M1 - XO) = E(M1 - XO) - [E(\text{heme1}) + E(XO)] + E_{\text{BSSE}} \quad (1)$$

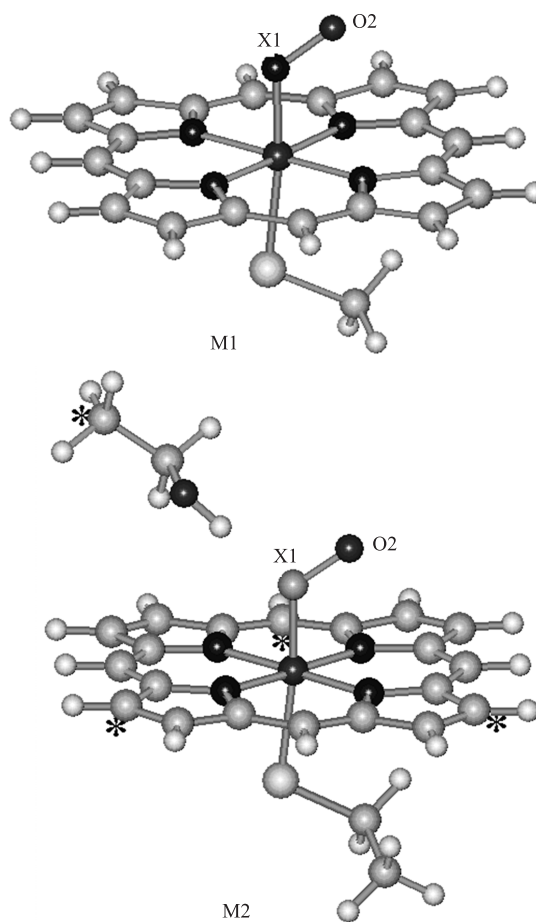


FIG. 2 The binding of diatomic molecule (XO) to the active site in M1 and M2, respectively.

and for the M2-XO system,

$$\Delta E(M2 - XO) = E(M2 - XO) - [E(\text{heme2}) + E(\text{ser}) + E(XO)] + E_{\text{BSSE}} \quad (2)$$

where heme1 refers to the modeled heme group with cystein modeled as $-\text{SCH}_3$, heme2 refers to the modeled heme group with cystein modeled as $-\text{SCH}_2\text{CH}_3$, and E_{BSSE} refers the energy of the BSSE.

IV. RESULTS AND DISCUSSION

A. Geometries

Two binding modes (Fe-XO and Fe-OX) were considered, but only the Fe-XO binding mode is discussed since the Fe-XO binding mode is more stable than the Fe-OX binding one. The main optimized geometrical parameters are listed in Table I. Collman *et al.* [12,18] have noted that the Fe-CO bond is linear with an Fe-C-O angle close to 180°, whereas Fe-O₂ is bent, with an Fe-O-O angle around 120°, which is in accord with the current results as listed in Table I. Table I also

TABLE I Important bond lengths d (Å) and bond angles ($^\circ$) as well as the binding energies ΔE (kJ/mol) of various models

	$d(\text{Fe}-\text{X})$	$d(\text{X}-\text{O})$	$\angle\text{Fe}-\text{X}-\text{O}$	$d(\text{O}-\text{H})$	$d(\text{H}\cdots\text{O}(\text{X}))$	$\angle\text{O}-\text{H}\cdots(\text{O})\text{X}$	ΔE
M1-O ₂	1.770 (1.89) ^a	1.291 (1.35)	122.8 (118.1)	—	—	—	-167.44
M1-CO	1.771 (1.80)	1.159 (1.17)	179.5 (179.9)	—	—	—	-75.93
M1-NO	1.778 (1.82)	1.191 (1.20)	139.6 (142.0)	—	—	—	-75.64
M2-O ₂	1.778	1.297	123.1	0.979	1.974	176.8	-190.71
M2-CO	1.756	1.165	175.8	0.972	2.030	158.1	-90.88
M2-NO	1.831	1.203	135.9	0.977	2.119	168.1	-100.46
	$d(\text{Fe}-\text{O})$	$d(\text{O}-\text{X})$	$\angle\text{Fe}-\text{O}-\text{X}$	$d(\text{O}-\text{H})$	$d(\text{H}\cdots\text{O}(\text{X}))$	$\angle\text{O}-\text{H}\cdots(\text{O})\text{X}$	ΔE
M1-OC	2.156	1.281	123.1	—	—	—	-46.25
M1-ON	2.514	1.184	129.8	—	—	—	-45.50
M2-OC	2.027	1.142	176.5	—	—	—	-54.33
M2-ON	1.944	1.253	128.4	0.978	1.961	174.9	-62.87

^a The values in bracket are cited from Ref.[4].

lists the parameters calculated by Blomberg *et al.* [4], and it is clear that those outcomes in good accord with the ones of this study: the differences of bond lengths are no larger than 0.12 Å and those of bond angles are less than 4°. The XO π^* orbital are empty for CO, allowing backdonation of electrons from the d orbital of Fe, while NO and O₂ have one and two electrons in their π^* orbital, respectively, which induce Fe-XO bending to avoid an antibonding interaction. The bond length of XO elongates from M1 to M2. The binding angle Fe-O-O in O₂ complex increases on going from M1 to M2, while the corresponding angle Fe-C-O and Fe-N-O in CO and NO complexes decreases from M1 to M2, which can be seen from Table I.

The binding angle Fe-X-O increases on going from O₂ to CO in the two different models and the O₂ complex is the most stable of all. The most obvious difference is the structure of the M2-CO complex: the H-bond angle in it is 158.1° while in the other two it is 168.1° and 176.8°, respectively (see Table I). The C-Fe bond is 1.756 Å in M2-CO while it is 1.771 Å in M1-CO. The difference is due to the atoms forming an H-bond. In O₂ and NO complex, the H-bond can form between the O-H of methanol and the X atom of NO or O₂, while this is not the case in CO because the C atom cannot form an H-bond, and the H-bond must be formed using the O atom of CO. This results in the longer X-Fe bond distance in CO than in the other two, and the H-bond angles in CO are different from the other two.

Variations in the internal porphyrin structure are not detailed here since these are minor and the Fe atom is nearly in the same plane as porphyrin.

B. Frequency analysis

Frequency analysis was performed at the B3LYP/6-31G(d) level and the results indicate that all the com-

plexes have no imaginary frequencies and thus are local minima. As is well known, the CO frequency diminishes by about 200 cm⁻¹ and the $\nu_{\text{C-O}}$ infrared intensity is greatly augmented from its gas phase value when bound to heme [29]. The calculated results indicate that the $\nu_{\text{C-O}}$ stretching vibration is 2040.30 cm⁻¹ in M1-CO complex and it decreases by 167.78 cm⁻¹ as compared with that of the CO monomer, which is in accord with the results of Park [29]. The IR intensity in the M1-CO complex is 766.5 km/mol while that in the CO monomer is 67.9 km/mol, so it can be seen that the $\nu_{\text{C-O}}$ infrared intensity is significantly augmented. The $\nu_{\text{C-O}}$ stretching vibration in monomer O₂ is 1643.49 cm⁻¹, and it decreases to 1254.30 cm⁻¹ in M1-O₂ complex. Like the $\nu_{\text{C-O}}$ stretching vibration, the IR intensity of $\nu_{\text{O-O}}$ is obviously augmented from 0.0 km/mol in O₂ monomer to 67.9 km/mol in M1-O₂ complex. The stretching vibrational frequency of $\nu_{\text{N-O}}$ in M2-NO is 1695.29 cm⁻¹, and the decrease is 294.69 cm⁻¹ as compared with that of the monomer NO. The IR intensity of $\nu_{\text{N-O}}$ is also largely broadened. From all the above mentioned, it can be seen that the $\nu_{\text{X-O}}$ stretching vibration frequency is blue-shifted as complexed with heme and the IR intensity is greatly augmented at the same time. The $\nu_{\text{Fe-C}}$ is 501.31 cm⁻¹ in M1-CO, the $\nu_{\text{Fe-N}}$ is 418.62 cm⁻¹ in M1-NO, and the $\nu_{\text{Fe-O}}$ is 627.58 cm⁻¹ in M1-O₂, which indicates that the larger the $\nu_{\text{Fe-X}}$ is, the more stable the complex is.

As we can see from Table II, the stretching vibration of C-O is 2040.30 cm⁻¹ in M1-CO, and 2003.72 cm⁻¹ in M2-CO, and the corresponding frequency shifts are 167.78 and 204.36 cm⁻¹, respectively, in the two models as compared with the corresponding vibrational frequency in monomer CO. Likewise, the frequency shifts of $\nu_{\text{O-O}}$ are 389.19 cm⁻¹ in M1-O₂ and 407.78 cm⁻¹ in M2-O₂ and that of $\nu_{\text{N-O}}$ are 295.69 cm⁻¹ in M1-NO and 341.31 cm⁻¹ in M2-NO, respectively. It can be seen from Table II that the infrared intensity of $\nu_{\text{X-O}}$ also increased from M1-XO to M2-XO except for the

TABLE II Calculated harmonic frequencies (cm⁻¹) and frequency shifts for various models

	$\nu_{\text{Fe-XO}}$	$\nu_{\text{X-O}}$	$\Delta\nu_{\text{X-O}}$	$\nu_{\text{O-H}}$	$\Delta\nu_{\text{O-H}}$
M1-CO	501.31 (2.34) ^a	2040.30 (766.47)	167.8	—	—
M1-NO	418.62 (47.81)	1695.29 (1113.89)	295.7	—	—
M1-O ₂	627.58 (14.42)	1254.30 (375.29)	389.2	—	—
M2-CO	522.28 (0.53)	2003.72 (939.37)	204.4	3729.41 (168.60)	-20.18
M2-NO	415.34 (2.06)	1649.67 (648.46)	341.3	3625.10 (393.71)	-124.49
M2-O ₂	627.37 (74.04)	1235.71 (417.03)	407.8	3601.83 (652.59)	-147.76

^a The values in brackets are IR intensities (km/mol).

TABLE III NBO charges (e) of selected atoms in various models.

	Fe	X1	O ₂	S	H(ser)	O(ser)
M1-CO	1.225	0.357	-0.528	-0.477	—	—
M1-NO	1.344	-0.027	-0.283	-0.460	—	—
M1-O ₂	1.358	-0.209	-0.226	-0.388	—	—
M2-CO	1.226	0.370	-0.559	-0.481	0.490	-0.782
M2-NO	1.417	-0.276	-0.271	-0.360	0.505	-0.788
M2-O ₂	1.350	-0.165	-0.303	-0.367	0.497	-0.791

NO complex. The variation of $\nu_{\text{Fe-XO}}$ vibrational frequency in the M1 model and M2 model are slight as XO=NO or O₂, while it changes by about 20 cm⁻¹ in CO complexes, which indicates that the near serine residue affects the CO complex greatly, which is consistent with the larger geometrical variation caused to the CO complex.

When a positive charge approaches the CO (such as the H atom of methanol), the π^*_{CO} orbital are energetically stabilized. As they get closer in energy to the Fe-d orbital, the back-bonding increases, and as a consequence, the CO frequency decreases [30]. Therefore, when considering the serine residue, the stretching vibration of C—O decreases from 2040.30 cm⁻¹ to 2003.72 cm⁻¹, which can be seen from Table II.

The O—H vibrational frequency $\nu_{\text{O-H}}$ is 3729.41, 3625.10, and 3601.83 cm⁻¹ in M2-CO, M2-NO, and M2-O₂, respectively, while it is 3749.58 cm⁻¹ in methanol. Therefore, it can be seen that as the frequency shifts increased and the hydrogen bond strengthened from CO to O₂; that is, the larger the frequency shifts of $\nu_{\text{O-H}}$, the more stable the complex. From data listed in Table II, one can also note that the frequency shifts are correlated with the bond length increase of the O—H bond; that is, the larger the elongation of bond O—H, the larger the frequency shifts of $\nu_{\text{O-H}}$.

C. Energetic properties

As to M2-XO complexes, the binding energy of XO to heme decreased from CO to O₂, while the stability sequence changed to NO<CO<O₂ for the M1-XO complex. The binding energies of CO and NO are similar

to those of M1-XO and M2-XO complexes. Stabilization energies listed in Table I show that the effect of serine residue to CO binding heme complex is weaker than that of NO and O₂ complexes. The binding energy of M1-CO is -75.93 kJ/mol while that involving methanol (M2-CO) is only -14.94 kJ/mol more stable. However, the stabilization energy caused by methanol is -23.27 and -24.82 kJ/mol for the O₂ and NO complex. It is clear that the O₂ complex is the most stable one of the three, while the binding energies of CO and NO complexes are similar and are more unstable by 83.72 kJ/mol or so than the O₂ complex. When bound to Fe(II) the XO molecule can become significantly polar and it can interact with the nearby methanol. The p orbital energy of XO increases from CO to O₂, thus the extent of backbonding electron transfer to XO via the π^* orbital increases in the order of CO<NO<O₂. Therefore, M2-O₂ is the most stable one of the three and the serine residue near the heme enforced the binding of XO to heme.

D. Charge distributions and bonding analysis

From an analysis of the atomic charges evaluated by the NBO method, one can easily see that the charge difference between M1-CO and M2-CO is inconspicuous. However, comparing the charge of XO of the three different complexes, one can find that the charge of CO is remarkably different from that of O₂ and NO. From Table III, we can see that the charge of O1 is -0.209e and -0.276e in M1-O₂ and M2-O₂, and that of N1 is -0.027e and -0.165e in M1-NO and M2-NO, while the corresponding C atom charge is 0.357e and 0.370e in

M1-CO and M2-CO, respectively. Correspondingly, the O atom in CO complex has much lower charge as compared with that in O₂ and NO complexes.

The charge transfer from the lone pair of O1 to the antibonding orbital of O–H in methanol stabilizes the M2-O₂ complex by –39.47 kJ/mol, while the interaction between the lone pair of O₂ and the antibonding orbital of O–H contributes –20.34 kJ/mol to the stabilization energy of M2-CO, and the charge transfer from the lone pair of N1 to the antibonding orbital of O–H stabilizes the M2-NO complex. This indicates that the hydrogen bond between the XO diatomic molecule and serine residue is appreciably stronger in the O₂ complex than in the CO complex.

V. CONCLUSION

In this work, the binding of the diatomic CO, NO, and O₂ to P450 ferrous heme were calculated in two different models. It is worth considering whether the other amino acid residues have the synergistic effect or not, and the authors are trying to extend the computing range in order to consider more amino acid residues than in the present models. From the obtained results we can draw the following conclusions:

(i) Geometries of the different XO complexes are alike in the two models: the CO binds nearly linearly to heme, while NO and O₂ bind to heme with bond angles Fe–X–O of 140° and 120° or so, respectively. The Fe–XO binding mode is more stable than the Fe–OX binding one in each model.

(ii) Frequency analysis suggests that the ν_{X-O} stretching vibrational frequency decreased as XO complexed with heme and the decrease in the M2 models is less significant than in M1. The IR intensity is greatly augmented at the same time.

(iii) Stabilization energies of various models indicate that the O₂ binding complex is the most stable one among the three complexes, while the CO and NO binding complexes have similar stabilization energies in M1 and M2.

(iv) A hydrogen bond formed between the H atom of O–H in serine and the X atom of O₂ and NO molecules, while it formed between the O atom of CO and the H atom of O–H in serine in the CO complex. The frequency shifts of ν_{O-H} in M2-XO complex as compared with that in methanol diminished from CO to O₂ through NO.

VI. ACKNOWLEDGMENTS

This work was supported by the National Natural Science Foundation of China (No.20373034), the China Postdoctoral Science Foundation (No.20060400991), and the Shandong Province Postdoctoral Science Foundation of (No.200601007).

- [1] P. R. Ortiz de Montellano, *Cytochrome P-450: Structure, Mechanism, and Biochemistry*, New York: Plenum Press, (1986).
- [2] D. Vitkup, G. A. Petsko, and M. Karplus. *Nature Struct. Biol.* **4**, 202 (1997).
- [3] J. S. Olson and G. N. Jr. Philips, *J. Biol. Chem.* **271**, 17593 (1996).
- [4] L. M. Blomberg, M. R. A. Blomberg, and P. E. M. Siegbahn, *J. Inorg. Biochem.* **99**, 949 (2005).
- [5] F. De Angelis, A. A. Jarzecki, R. Car, and T. G. Spiro, *J. Phys. Chem. B* **109**, 3065 (2005).
- [6] E. Sigfridsson and U. Ryde, *J. Inorg. Biochem.* **91**, 101 (2002).
- [7] T. G. Spiro and A. A. Jarzecki, *Curr. Opin. Chem. Biol.* **5**, 715 (2001).
- [8] C. Rovira and M. Parrinello, *Biophysical J.* **78**, 93 (2000).
- [9] S. Franzen, *Proc. Natl. Acad. Sci. USA* **99**, 16754 (2002).
- [10] M. Tsuda, W. A. Diño, H. Nakanishi, and H. Kasai, *Chem. Phys. Lett.* **402**, 71 (2005).
- [11] K. P. Jensen and U. Ryde, *J. Biol. Chem.* **279**, 14561 (2004).
- [12] J. P. Collman, J. I. Brauman, T. R. Halbert, and K. S. Suslick, *Proc. Natl. Acad. Sci. USA* **73**, 3333 (1976).
- [13] K. M. Vogel, P. M. Kozlowski, M. Z. Zgierski, and T. G. Spiro, *J. Am. Chem. Soc.* **121**, 9915 (1999).
- [14] C. Rovira and M. Parrinello, *Int. J. Quant. Chem.* **80**, 1172 (2000).
- [15] T. G. Spiro, M. Z. Zgierski, and P. M. Kozlowski, *Coord. Chem. Rev.* **219**, 923 (2001).
- [16] F. Torrents, *Polyhedron* **22**, 1091 (2003).
- [17] E. Tangen, A. Svadberg, and A. Ghosh, *Inorg. Chem.* **44**, 7802 (2005).
- [18] J. P. Collman, *Inorg. Chem.* **36**, 5145 (1997).
- [19] D. Leys, C. G. Mowat, K. J. Mclean, A. Richmond, S. K. Chapman, M. D. Walkinshaw, and A. W. Munro, *J. Biol. Chem.* **278**, 5141 (2003).
- [20] R. Vianello, B. Kovačević, G. Ambrožič, J. Mavri, and Z. B. Maksić, *Chem. Phys. Lett.* **400**, 117 (2004).
- [21] A. Warshel, *Computer Modelling of Chemical Reactions in Enzymes and Solutions*, New York: Wiley, (1991).
- [22] W. W. Cleland and M. M. Kreevoy, *Science* **264**, 1887 (1994).
- [23] W. W. Cleland and M. M. Kreevoy, *Science* **269**, 104 (1995).
- [24] M. Strajbl and J. Florian, *Theor. Chem. Acc.* **99**, 166 (1998).
- [25] T. Kamachi and K. Yoshizawa, *J. Am. Chem. Soc.* **125**, 4652 (2003).
- [26] H. Lin, J. C. Schöneboom, S. Cohen, S. Shaik, and W. Thiel, *J. Phys. Chem. B* **108**, 10083 (2004).
- [27] V. Guallar, M. H. Baik, S. J. Lippard, and R. A. Friesner, *Proc. Natl. Acad. Sci. USA* **100**, 6998 (2003).
- [28] S. Erkoc and F. Erkoc, *THEOCHEM.* **546**, 175 (2001).
- [29] E. S. Park, S. S. Andrews, R. B. Hu, and S. G. Boxer, *J. Phys. Chem. B* **103**, 9813 (1999).
- [30] C. Rovira, B. Schulze, M. Eichinger, J. D. Evanseck, and M. Parrinello, *Biophys. J.* **81**, 435 (2001).